Synthesis and Structure of New Phosphido-bridged Iron–Cobalt and Iron–Nickel Nitrosyl Complexes

CHUNG-NIN CHAU, ANDREW WOJCICKI*

Department of Chemistry, The Ohio State University, Columbus, OH 43210 (U.S.A.)

MARIO CALLIGARIS**

Dipartimento di Chimica Generale, Università di Pavia, 27100 Pavia (Italy)

and GIORGIO NARDIN

Dipartimento di Scienze Chimiche, Università di Trieste, 34127 Trieste (Italy)

(Received July 31, 1989; revised October 12, 1989)

Abstract

The dianion of $Li_2[(NO)_2\overline{Fe(\mu\text{-}PPh_2)(\mu\text{-}NO)}Fe(NO)(PPh_2)]$ reacts with each of $CpCo(CO)I_2$ and $Ni(dppe)I_2$ (dppe $\equiv Ph_2PCH_2CH_2PPh_2$) in THF solution over the temperature range −78 to 25 °C to afford new heteronuclear metal complexes, $(NO)_2\overline{Fe(\mu\text{-}PPh_2)(\eta^2\text{-}(Co,P)\text{-}\mu\text{-}Co(Cp)(CO)PPh_2)}Fe(NO)_2$ (**1**) and $(NO)_2Fe(1\text{-}(\mu\text{-}PPh)\text{-}2\text{-}(PPh_2)C_2H_4)_2Ni$ (**2**), respectively. The structures of the products were determined by X-ray crystallography. Crystals of **1** are orthorhombic, space group $P2_12_12_1$, with a = 11.387(5), b = 12.075(5), c = 22.360(8) Å, Z = 4. Crystals of **2** are monoclinic, space group $P2_1/n$, with a = 12.222(4), b = 13.843(4), c = 23.210(9) Å, β = 104.01(4)°, Z = 4. The structures were refined to R = 0.056, R_w = 0.056 and R = 0.035, R_w = 0.036 for **1** and **2**, respectively, by using 2481 and 5457 independent reflections. The structure of **1** is characterized by an asymmetric triangular arrangement of the metal atoms with two PPh_2 groups bridging the Fe(1), Fe(2) and Co, Fe(2) atom pairs. The latter pair is at the non-bonding distance of 3.796(1) Å. The Fe(1)–Fe(2) and Co–Fe(1) bond lengths are 2.797(1) and 2.569(1) Å, respectively. In **2**, one $Fe(NO)_2$ group is bonded to a Ni atom through a single bond supported by the bridging of two phosphido ligands, $PPh(CH_2CH_2PPh_2)$, whose phosphine groups complete the Ni coordination. The structure of the $FeNiP_2$ ring is planar with a Fe–Ni distance of 2.6166(4) Å.

Introduction

In the course of our investigations of reduction chemistry of binuclear metal–μ-phosphido complexes [1], we observed that treatment of $Fe_2(NO)_4(\mu\text{-}PPh_2)_2$ with 1 or 2 eq. of $MBEt_3H$ (M = Li, Na, K) proceeds with cleavage of one Fe–P bond to afford $M[(NO)_2\overline{Fe(\mu\text{-}PPh_2)(\mu\text{-}NO)}Fe(NO)(PPh_2H)]$ [2] (eqn. (1)).

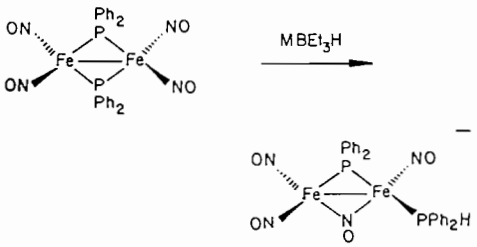

(1)

The product monoanion can be deprotonated by n-BuLi at low temperatures to a very reactive dianion, $[(NO)_2\overline{Fe(\mu\text{-}PPh_2)(\mu\text{-}NO)}Fe(NO)(PPh_2)]^{2-}$ (eqn. (2)).

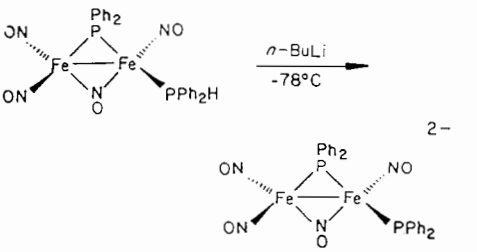

(2)

The dianion undergoes facile alkylation of the terminal PPh_2 ligand by 1 eq. of RI (R = Me, Et, CH_2Ph, etc.); however, with 2 eq. of RI fragmentation of the binuclear structure occurs to give $Fe(NO)_2(PPh_2R)_2$. Such fragmentation can be prevented by using $RCHI_2$ (R = H, Me) in place of RI. The hydrocarbon group RCH adds to the terminal PPh_2 phosphorus and to the $Fe(NO)_2$ iron to generate an η^2-(C,P)-μ-$CH(R)PPh_2$ bridging ligand in the binuclear complex $(NO)_2\overline{Fe(\mu\text{-}PPh_2)(\eta^2\text{-}(C,P)\text{-}\mu\text{-}CH(R)PPh_2)}Fe(NO)_2$ [3] (eqn. (3)).

*Author to whom correspondence should be addressed.

**Author to whom correspondence concerning the X-ray crystallographic analyses should be addressed.

0020-1693/90/$3.50

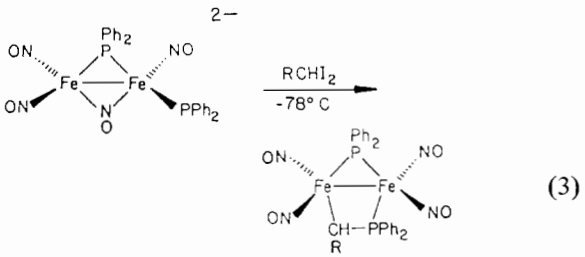

(3)

One may envisage an extension of this chemistry to the synthesis of trinuclear metal complexes by consideration of Hoffmann's isolobal analogy [4]. The fragment RCH is regarded as being isolobal with various metal-containing species, e.g. $Fe(CO)_4$ and CpCo(CO). Thus, the use of metal diiodo complexes, L_nMI_2, in place of $RCHI_2$ in the reaction in eqn. (3), may lead to the formation of η^2-*(M,P)*-μ-M(L_n)PPh_2-bridged complexes, $(NO)_2Fe(\mu\text{-}PPh_2)(\eta^2\text{-}(M,P)\text{-}\mu\text{-}M(L_n)PPh_2)Fe(NO)_2$, e.g. $(NO_2Fe(\mu\text{-}PPh_2)(\eta^2\text{-}(Co,P)\text{-}\mu\text{-}Co(Cp)(CO)PPh_2)Fe(NO)_2$ (**1**) when $CpCo(CO)I_2$ is employed. If successful, this approach would afford a new synthetic methodology for a series of related heterotrinuclear Fe_2M clusters.

The study reported in this paper has been conducted in that vein. Specifically, we examined reactions of $Li[(NO)_2Fe(\mu\text{-}PPh_2)(\mu\text{-}NO)Fe(NO)(PPh_2)]$ with each of $CpCo(CO)I_2$, $Ni(dppe)I_2$ (dppe ≡ $Ph_2PCH_2CH_2PPh_2$) and Cp_2ZrI_2. Whereas the reaction with $CpCo(CO)I_2$ yielded the anticipated product, that with $Ni(dppe)I_2$ unexpectedly afforded the binuclear complex $(NO)_2Fe(1\text{-}(\mu\text{-}PPh)\text{-}2\text{-}(PPh_2)\text{-}C_2H_4)_2Ni$ (**2**). No FeZr complexes could be isolated from the reaction with Cp_2ZrI_2. Both heteronuclear products were characterized by spectroscopy and X-ray crystallography.

Experimental

General Procedures and Measurements

All reactions and manipulations of air-sensitive compounds were carried out under an atmosphere of purified N_2 by using standard procedures [5]. Elemental analyses were determined by Galbraith Laboratories, Inc., Knoxville, TN. Chromatographic separations and purifications were effected on columns packed with alumina (*c.* 150 mesh, 6% H_2O). Melting points were measured *in vacuo* on a Thomas-Hoover melting point apparatus and are uncorrected. Infrared (IR) spectra were recorded on a Perkin-Elmer Model 337 or 283B spectrophotometer and were calibrated with polystyrene. ^1H NMR spectra were obtained on a Varian Associates EM 360L spectrometer. ^{31}P NMR spectra were recorded on a Bruker HX-90 spectrometer at 36.43 MHz in the Fourier transform mode. Chemical shifts are given with reference to 85% H_3PO_4 and are reproducible to ±0.1 ppm. Mass spectra were obtained by use of the fast atom bombardment (FAB) technique on a Kratos MS-30 spectrometer by Mr C. R. Weisenberger.

Materials

THF was distilled from Na and benzophenone under an atmosphere of N_2 immediately before use. Other solvents were purified according to procedures described by Perrin *et al.* [6].

$LiBEt_3H$ (1.0 M in THF) and n-BuLi (1.6 M in hexanes) were obtained from Aldrich. The complex $CpCo(CO)_2$ was purchased from Strem, and Cp_2ZrCl_2 from Alfa, for the preparation of the respective diiodides $CpCo(CO)I_2$ [7] and Cp_2ZrI_2 [8]. Other reagents were obtained from various commercial sources and used as received. $Ni(dppe)I_2$ (dppe ≡ $Ph_2PCH_2CH_2PPh_2$) [9] and $Fe_2(NO)_4(\mu\text{-}PPh_2)_2$ [10] were prepared according to the literature.

Reaction of $Li_2[(NO)_2Fe(\mu\text{-}PPh_2)(\mu\text{-}NO)Fe(NO)(PPh_2)]$ with $CpCo(CO)I_2$

A solution of the title iron complex was prepared by treatment of 0.50 g (0.83 mmol) of $Fe_2(NO)_4(\mu\text{-}PPh_2)_2$ in 50 ml of THF with 0.83 ml (0.83 mmol) of 1.0 M solution of $LiBEt_3H$ in THF at 25 °C, cooling to −78 °C, and addition of 0.55 ml (0.88 mmol) of 1.6 M solution of n-BuLi in hexanes [2]. After 0.60 g (1.48 mmol) of solid $CpCo(CO)I_2$ had been introduced with stirring, the reaction mixture was allowed to warm to room temperature over 10 h. The muddy brown mixture was evaporated to dryness, and the residue was chromatographed on a 40 × 1 cm column of alumina. Elution with petroleum ether removed from the column a narrow green band (IR ν(NO) 1750s, 1705s cm^{-1}; $^{31}P\{^1H\}$ NMR δ 182.99 ppm), which could not be completely characterized because of a low yield. Elution with 5:95 diethyl ether/petroleum ether then removed from the column a major dark brown band which yielded, after evaporation to dryness, 0.15 g (24%) of $(NO)_2Fe(\mu\text{-}PPh_2)(\eta^2\text{-}(Co,P)\text{-}\mu\text{-}Co(Cp)(CO)PPh_2)Fe(NO)_2$ (**1**), melting point (m.p.) 75 °C (dec.). IR ($CHCl_3$) ν(CO) 1980s, ν(NO) 1750s, 1730s cm^{-1}; ^1H NMR (acetone-d_6) δ 7.50br (4Ph), 5.24s (Cp) ppm; $^{31}P\{^1H\}$ NMR (THF) δ 229.44d (Fe–P–Fe), 101.81d ($^2J(^{31}P^{31}P)$ = 49.4 Hz, Fe–P–Co) ppm; mass spectrum, *m/e* 754 (M^+). *Anal.* Found: C, 49.77; H, 3.98. Calc.: C, 47.74; H, 3.22%.

Further elution, with THF, produced a red band which was collected and evaporated to dryness to give 0.08 g (*c.* 20%) of $Fe_2(NO)_4(\mu\text{-}PPh_2)_2$, identified by its IR ν(NO) spectrum [2].

Reaction of $(NO)_2Fe(\mu\text{-}PPh_2)(\eta^2\text{-}Co,P)\text{-}\mu\text{-}Co(Cp)(CO)PPh_2)Fe(NO)_2$ (1) with PPh_3

A solution of **1** (0.30 g, 0.39 mmol) in THF (20 ml) was treated with PPh_3 (0.20 g, 0.76 mmol),

also in THF (10 ml), at 25 °C. The resulting deep brown solution was stirred for 4 h, during which time $Fe_2(NO)_4(\mu\text{-}PPh_2)_2$ (0.15 g) precipitated. Examination of the reaction solution by ^{31}P NMR spectroscopy revealed no PPh_3-containing derivative of **1**.

Reaction of $Li_2[(NO)_2\overline{Fe(\mu\text{-}PPh_2)(\mu\text{-}NO)}\overline{Fe(NO)}(PPh_2)]$ with $Ni(dppe)I_2$

A solution of the title iron complex was prepared as described for the corresponding reaction with $CpCo(CO)I_2$. To this solution was added 0.70 g (0.84 mmol) of solid $Ni(dppe)I_2$ with stirring at −78 °C. The resulting mixture was allowed to warm to room temperature over 10 h. The purple reaction mixture was then evaporated to dryness, and the residue was chromatographed on alumina. Elution with petroleum ether removed from the column a very narrow brown band which contained insufficient material for characterization. Elution with 5:95 diethyl ether/petroleum ether then removed a deep purple band which was collected and evaporated to dryness to give 0.2 g (20% yield) of $(NO)_2\overline{Fe(1\text{-}(\mu\text{-}PPh)\text{-}2\text{-}(PPh_2)C_2H_4)_2}\overline{Ni}$ (**2**). IR (THF) ν(NO) 1760s, 1710s cm^{-1}; $^{31}P\{^1H\}$ NMR (THF) δ 206.66t (μ-P), 39.86t ($^2J(^{31}P^{31}P) = 10$ Hz, CH_2PPh_2) ppm. This complex is sometimes obtained contaminated with $Ni(dppe)I_2$ ($^{31}P\{^1H\}$ NMR δ 80.44 ppm), which is difficult to remove by column chromatography. Further elution, with THF, afforded a red band of $Fe_2(NO)_4(\mu\text{-}PPh_2)_2$, from which 0.05 g (10%) of the compound was obtained after solvent removal.

Reaction of $Li_2[(NO)_2\overline{Fe(\mu\text{-}PPh_2)(\mu\text{-}NO)}\overline{Fe(NO)}(PPh_2)]$ with Cp_2ZrI_2

A solution of the title iron complex, prepared as described for the previous reactions, was treated with an equimolar amount (0.40 g, 0.84 mmol) of solid Cp_2ZrI_2 at −78 °C. The mixture was allowed to warm to *c.* 25 °C over 10 h and filtered, at which point a ^{31}P NMR spectrum revealed the presence of several resonances, the major one being that of $Fe_2(NO)_4(\mu\text{-}PPh_2)_2$ (δ 261.5 ppm). Attempted chromatography on alumina afforded no product

TABLE 1. Crystal data, data collection and refinement of **1** and **2**

Complex	**1**	**2**
Molecular formula	$Fe_2CoC_{30}H_{25}N_4O_5P_2$	$FeNiC_{40}H_{38}N_2O_2P_4$
Molecular weight	754.1	718.3
Crystal system	orthorhombic	monoclinic
Space group	$P2_12_12_1$	$P2_1/n$
a (Å)	11.387(5)	12.222(4)
b (Å)	12.075(5)	13.843(4)
c (Å)	22.360(8)	23.210(9)
β (°)		104.01(4)
V (Å^3)	3074(2)	3810(2)
Z	4	4
D_{calc} (g cm^{-3})	1.629	1.425
F(000)	1536	1472
Absorption coefficient (Mo Kα) (cm^{-1})	16.1	10.8
Crystal size (mm)	0.35 × 0.23 × 0.41	0.20 × 0.22 × 0.70
Diffractometer	Enraf-Nonius CAD4	Enraf-Nonius CAD4
Temperature (°C)	21 ± 1	21 ± 1
Radiation (λ, Å)	Mo Kα, 0.71069	Mo Kα, 0.71069
Monochromator	graphite	graphite
Scan type	$\omega/2\theta$	$\omega/2\theta$
Scan speed (° min^{-1})	variable (0.72–4)	variable (0.87–5)
2θ range (°)	5–56	6–56
Reflections measured	$+h, +k, +l$	$\pm h, +k, +l$
Orientation monitors[a]	3	3
Intensity monitors[b]	4	4
Transmission factors	0.850–0.999	0.875–0.999
Total no. reflections measured	3674	9124
No. reflections with $I > 3\sigma(I)$[c]	2481	5457
Data/parameter ratio	12.3	12.1
R[d]	0.056	0.035
R_w[e]	0.056	0.036
GOF[f]	2.63	1.65

[a]Measured after each 400 reflections; new orientation matrix if angular change >0.13. [b]Measured after each 3000 s. [c]Standard deviation from counting statistics. [d]$R = \Sigma\|\|F_o| - |F_c\|/\Sigma|F_o|$. [e]$R_w = [\Sigma w(|F_o| - |F_c|)^2/\Sigma wF_o^2]^{1/2}$; $w = 1$. [f]$GOF = [\Sigma w(|F_o| - |F_c|)^2/(m - n)]^{1/2}$; m = no. of observations, n = no. of variables.

other than $Fe_2(NO)_4(\mu\text{-}PPh_2)_2$ in a sufficient quantity for characterization.

Crystallographic Analyses of $(NO)_2\overline{Fe(\mu\text{-}PPh_2)(\eta^2\text{-}(Co,P)\text{-}\mu\text{-}Co(Cp)(CO)PPh_2)Fe(NO)_2}$ (1) and $(NO)_2\text{-}Fe(1\text{-}(\mu\text{-}PPh)\text{-}2\text{-}(PPh_2)C_2H_4)_2Ni$ (2)

Crystals were grown from diethyl ether/hexane solutions. Lattice constants were determined by a least-squares refinement of 25 reflections, accurately centered on an Enraf-Nonius CAD4 diffractometer. A summary of the crystal data and details of the intensity data collection and refinement are presented in Table 1. No significant change in intensities of control reflections was observed over the course of data collections. An empirical absorption correction was applied to observed data, based on the Ψ scans of four close-to-axial reflections. Both structures were solved by direct methods (MULTAN 80) and Fourier techniques. After anisotropic refinement, the calculated idealized positions of hydrogen atoms (0.96 Å from the parent C atoms) all occurred in positive electron density regions. Final full-matrix least-squares refinement, with the fixed contribution of hydrogen atoms ($B = 5$ Å^2), converged to $R = 0.056$ and $R = 0.035$ for **1** and **2**, respectively. Anisotropic temperature factors were assigned to the metal and phosphorus atoms only in **1**, and to all non-hydrogen atoms in **2**. Neutral-atom scattering factors, including anomalous dispersion, were taken from the literature [11]. All computations were carried out on a PDP 11/44 computer, using the SDP program system [12]. Final positional and equivalent thermal parameters are given in Tables 2 and 3.

TABLE 2. Positional and equivalent thermal parameters of non-hydrogen atoms of 1 with e.s.d.s in parentheses

Atom	x	y	z	B (Å^2)[a]
Co	0.1433(1)	0.1448(1)	0.66022(6)	3.01(2)
Fe1	0.3685(1)	0.1416(1)	0.66666(7)	3.05(2)
Fe2	0.3653(1)	−0.0897(1)	0.66019(6)	2.78(2)
P1	0.5170(2)	0.0208(2)	0.6719(1)	2.83(5)
P2	0.2076(2)	−0.0052(2)	0.6159(1)	2.79(5)
O1	0.4229(9)	0.2838(8)	0.5718(4)	6.0(2)*
O2	0.381(1)	0.2454(9)	0.7790(5)	6.8(2)*
O3	0.4204(9)	−0.2351(8)	0.5662(4)	5.9(2)*
O4	0.2969(9)	−0.1754(9)	0.7724(5)	6.8(2)*
O5	0.1422(9)	0.0416(8)	0.7754(4)	5.7(2)*
N1	0.3973(8)	0.2183(8)	0.6088(4)	4.1(2)*
N2	0.3728(9)	0.1971(8)	0.7332(4)	4.4(2)*
N3	0.4001(8)	−0.1723(8)	0.6057(4)	3.9(2)*
N4	0.3230(8)	−0.1332(8)	0.7263(4)	4.1(2)*
C1	0.146(1)	0.084(1)	0.7292(5)	4.0(2)*
C2	0.6240(9)	0.0252(9)	0.6107(4)	3.2(2)*
C3	0.6631(9)	0.1247(9)	0.5882(5)	3.3(2)*
C4	0.740(1)	0.126(1)	0.5409(5)	4.3(2)*
C5	0.776(1)	0.032(1)	0.5149(6)	4.9(3)*
C6	0.741(1)	−0.067(1)	0.5368(6)	4.9(3)*
C7	0.663(1)	−0.072(1)	0.5852(5)	4.4(2)*
C8	0.6059(9)	0.0321(9)	0.7387(4)	3.1(2)*
C9	0.725(1)	0.0525(9)	0.7384(5)	4.1(2)*
C10	0.785(1)	0.072(1)	0.7907(6)	4.6(3)*
C11	0.729(1)	0.070(1)	0.8437(6)	4.6(2)*
C12	0.612(1)	0.045(1)	0.8456(6)	5.2(3)*
C13	0.550(1)	0.026(1)	0.7941(6)	4.6(2)*
C14	0.2346(8)	0.0171(8)	0.5354(4)	2.7(2)*
C15	0.349(1)	0.0333(9)	0.5136(5)	3.5(2)*
C16	0.369(1)	0.0573(9)	0.4544(5)	4.1(2)*
C17	0.277(1)	0.064(1)	0.4163(5)	4.5(3)*
C18	0.167(1)	0.046(1)	0.4361(6)	4.9(3)*
C19	0.144(1)	0.021(1)	0.4947(5)	4.2(2)*
C20	0.0940(9)	−0.1110(9)	0.6157(5)	3.3(2)*
C21	0.103(1)	−0.202(1)	0.5765(5)	4.3(2)*
C22	0.020(1)	−0.283(1)	0.5755(6)	4.7(3)*
C23	−0.074(1)	−0.281(1)	0.6148(6)	5.0(3)*
C24	−0.086(1)	−0.193(1)	0.6515(6)	4.9(3)*
C25	−0.003(1)	−0.1096(9)	0.6519(5)	3.9(2)*
C26	0.143(1)	0.311(1)	0.6303(6)	5.2(3)*
C27	0.100(1)	0.239(1)	0.5859(7)	6.6(4)*
C28	0.004(1)	0.190(1)	0.6078(7)	6.3(3)*
C29	−0.018(1)	0.224(1)	0.6647(7)	5.9(3)*
C30	0.072(1)	0.300(1)	0.6789(7)	6.3(3)*

[a]Starred atoms were refined isotropically. Anisotropically refined atoms are given in the form of the isotropic equivalent thermal parameter defined as: $4/3[a^2B(1,1) + b^2B(2,2) + c^2B(3,3) + ab(\cos\gamma)B(1,2) + ac(\cos\beta)B(1,3) + bc(\cos\alpha)B(2,3)]$.

TABLE 3. Positional and equivalent thermal parameters of non-hydrogen atoms of 2 with e.s.d.s in parentheses

Atom	x	y	z	B (Å^2)[a]
Ni	0.45740(3)	0.74215(3)	0.20918(2)	2.293(7)
Fe	0.57833(4)	0.58445(4)	0.23130(2)	2.984(9)
P1	0.61378(7)	0.72344(7)	0.18625(4)	2.92(2)
P2	0.52811(7)	0.86070(6)	0.26598(4)	2.60(2)
P3	0.31336(7)	0.71169(7)	0.13641(4)	2.74(2)
P4	0.41296(7)	0.62302(6)	0.25549(4)	2.57(2)
O1	0.5326(3)	0.4262(2)	0.1521(2)	7.36(9)
O2	0.7392(3)	0.5470(3)	0.3384(1)	6.57(9)
N1	0.5489(3)	0.4960(2)	0.1824(2)	4.28(7)
N2	0.6734(2)	0.5698(2)	0.2946(1)	3.85(7)
C1	0.7179(3)	0.8102(3)	0.2280(2)	3.52(8)
C2	0.6824(3)	0.8417(3)	0.2840(2)	3.47(7)
C3	0.2820(3)	0.5826(3)	0.1448(2)	3.63(8)
C4	0.2858(3)	0.5633(3)	0.2100(2)	3.58(8)
C5	0.6444(3)	0.7209(3)	0.1131(2)	3.90(8)
C6	0.6668(4)	0.6361(4)	0.0873(2)	6.1(1)
C7	0.6817(4)	0.6380(5)	0.0289(2)	8.3(1)
C8	0.6747(4)	0.7229(6)	−0.0016(2)	8.1(2)
C9	0.6557(4)	0.8060(5)	0.0245(2)	7.2(1)

TABLE 3. *(continued)*

Atom	*x*	*y*	*z*	*B* (Å^2)[a]
C10	0.6398(4)	0.8065(4)	0.0812(2)	5.4(1)
C11	0.4974(3)	0.8763(3)	0.3387(1)	3.29(7)
C12	0.3896(3)	0.8552(3)	0.3436(2)	3.63(8)
C13	0.3610(3)	0.8621(3)	0.3978(2)	4.72(9)
C14	0.4413(4)	0.8892(4)	0.4473(2)	5.8(1)
C15	0.5481(5)	0.9097(4)	0.4436(2)	6.2(1)
C16	0.5771(4)	0.9034(4)	0.3891(2)	5.0(1)
C17	0.5121(3)	0.9820(2)	0.2338(2)	2.98(7)
C18	0.4940(3)	0.9909(3)	0.1727(2)	3.98(8)
C19	0.4891(4)	1.0815(3)	0.1466(2)	5.3(1)
C20	0.4968(4)	1.1637(3)	0.1809(2)	6.2(1)
C21	0.5124(4)	1.1555(3)	0.2408(2)	5.8(1)
C22	0.5212(3)	1.0660(3)	0.2677(2)	4.56(9)
C23	0.3227(3)	0.7239(3)	0.0596(1)	3.63(8)
C24	0.2965(4)	0.8114(4)	0.0313(2)	5.4(1)
C25	0.3092(4)	0.8246(5)	−0.0266(2)	7.2(1)
C26	0.3487(4)	0.7528(6)	−0.0551(2)	7.9(2)
C27	0.3765(4)	0.6666(5)	−0.0272(2)	7.5(1)
C28	0.3641(4)	0.6513(4)	0.0299(2)	5.6(1)
C29	0.1762(3)	0.7655(3)	0.1356(1)	3.04(7)
C30	0.1648(3)	0.8299(3)	0.1784(2)	3.64(8)
C31	0.0599(3)	0.8674(3)	0.1793(2)	4.60(9)
C32	−0.0340(3)	0.8403(3)	0.1375(2)	4.9(1)
C33	−0.0243(3)	0.7767(4)	0.0943(2)	6.0(1)
C34	0.0799(3)	0.7389(4)	0.0927(2)	5.3(1)
C35	0.4042(3)	0.6092(2)	0.3320(1)	2.83(6)
C36	0.4989(3)	0.6325(3)	0.3773(2)	3.67(8)
C37	0.4958(4)	0.6225(4)	0.4360(2)	4.7(1)
C38	0.4000(4)	0.5893(4)	0.4511(2)	5.2(1)
C39	0.3068(3)	0.5674(4)	0.4071(2)	5.0(1)
C40	0.3073(3)	0.5776(3)	0.3475(2)	3.96(8)

[a]Anisotropically refined atoms are given in the form of the isotropic equivalent thermal parameter defined as: $4/3[a^2B(1,1) + b^2B(2,2) + c^2B(3,3) + ab(\cos\gamma)B(1,2) + ac(\cos\beta)B(1,3) + bc(\cos\alpha)B(2,3)]$.

TABLE 4. Selected bond distances (Å) and angles (°) for **1** with e.s.d.s in parentheses

Co–Fe1	2.569(1)	Fe2–P2	2.291(2)
Co–P2	2.191(2)	Fe2–N3	1.624(6)
Co–C1	1.708(7)	Fe2–N4	1.640(6)
Co–C26	2.111(9)	P1–C2	1.833(7)
Co–C27	2.072(11)	P1–C8	1.810(7)
Co–C28	2.047(10)	P2–C14	1.846(6)
Co–C29	2.079(9)	P2–C20	1.818(7)
Co–C30	2.088(10)	N1–O1	1.181(8)
Fe1–Fe2	2.797(1)	N2–O2	1.182(8)
Fe1–P1	2.236(2)	N3–O3	1.186(8)
Fe1–N1	1.625(7)	N4–O4	1.189(8)
Fe1–N2	1.633(6)	C1–O5	1.155(8)
Fe2–P1	2.198(2)		
Co–Fe1–Fe2	89.95(4)	Fe1–Fe2–P2	65.65(5)
Co–Fe1–P1	140.13(7)	Fe1–Fe2–N3	130.5(2)
Co–Fe1–N1	98.5(2)	Fe1–Fe2–N4	106.1(2)

(continued)

TABLE 4. *(continued)*

Co–Fe1–N2	94.3(3)	P1–Fe2–P2	113.39(7)
Fe2–Fe1–P1	50.28(5)	P1–Fe2–N3	105.7(2)
Fe2–Fe1–N1	122.0(2)	P1–Fe2–N4	108.6(2)
Fe2–Fe1–N2	117.2(2)	P2–Fe2–N3	98.1(2)
P1–Fe1–N1	105.1(2)	P2–Fe2–N4	107.6(2)
P1–Fe1–N2	101.4(2)	N3–Fe2–N4	123.5(3)
N1–Fe1–N2	119.1(3)	Fe1–Co–P2	71.30(5)
Fe1–Fe2–P1	51.50(5)	Fe1–Co–C1	85.6(3)
P2–Co–C1	92.7(3)	Co–P2–C14	112.1(2)
Fe1–P1–Fe2	78.22(6)	Co–P2–C20	110.1(2)
Fe1–P1–C2	116.4(2)	C14–P2–C20	102.7(3)
Fe1–P1–C8	114.6(2)	Fe1–N1–O1	171.6(6)
C2–P1–C8	104.0(3)	Fe1–N2–O2	174.0(7)
Fe2–P2–Co	115.8(1)	Fe2–N3–O3	176.8(6)
Fe2–P2–C14	110.8(2)	Fe2–N4–O4	173.0(6)
Fe2–P2–C20	104.2(2)	Co–C1–O5	176.5(8)

TABLE 5. Selected bond distances (Å) and angles (°) for **2** with e.s.d.s in parentheses

Fe–Ni	2.6166(4)	P2–C17	1.828(3)
Fe–P1	2.281(1)	P3–C23	1.822(3)
Fe–P4	2.288(1)	P3–C29	1.830(3)
Fe–N1	1.650(3)	P4–C4	1.849(3)
Fe–N2	1.650(3)	P4–C35	1.814(3)
Ni–P1	2.120(1)	O1–N1	1.183(3)
Ni–P2	2.151(1)	O2–N2	1.177(3)
Ni–P3	2.166(1)	C1–C2	1.530(4)
Ni–P4	2.110(1)	C3–C4	1.526(4)
P1–C1	1.845(3)		
P1–C5	1.825(3)		
P2–C2	1.849(3)		
P2–C11	1.828(3)		
Ni–Fe–P1	50.74(2)	Fe–P1–Ni	72.85(2)
Ni–Fe–P4	50.42(2)	Fe–P1–C1	119.5(1)
Ni–Fe–N1	117.8(1)	Fe–P1–C5	121.0(1)
Ni–Fe–N2	121.3(1)	Ni–P1–C1	109.74(9)
P1–Fe–P4	101.11(3)	Ni–P1–C5	129.5(1)
P1–Fe–N1	110.2(1)	C1–P1–C5	103.3(1)
P1–Fe–N2	109.93(9)	Ni–P2–C2	105.47(9)
N1–Fe–N2	120.8(1)	Ni–P2–C11	120.9(1)
Fe–Ni–P1	56.40(2)	Ni–P2–C17	117.60(9)
Fe–Ni–P2	113.10(2)	C2–P2–C11	103.5(1)
Fe–Ni–P3	107.73(2)	C2–P2–C17	103.0(1)
Fe–Ni–P4	56.69(2)	C11–P2–C17	104.0(1)
P1–Ni–P2	89.67(3)	Ni–P3–C3	104.87(9)
P1–Ni–P3	113.10(3)	Ni–P3–C23	120.90(9)
P1–Ni–P4	113.03(3)	Ni–P3–C29	119.91(9)
P2–Ni–P3	139.17(3)	C3–P3–C23	104.9(1)
P2–Ni–P4	113.51(3)	C3–P3–C29	100.5(1)
P3–Ni–P4	89.10(3)	C23–P3–C29	103.1(1)
Fe–P4–Ni	72.89(2)	Fe–N1–O1	173.1(3)
Fe–P4–C4	115.2(1)	Fe–N2–O2	171.4(3)
Fe–P4–C35	118.69(9)	P1–C1–C2	109.3(2)
Ni–P4–C4	110.0(1)	P2–C2–C1	109.4(2)
Ni–P4–C35	131.65(9)	P3–C3–C4	108.4(2)
C4–P4–C35	105.7(1)	P4–C4–C3	108.0(2)

TABLE 6. Equations of planes angles between planes (°), and displacements of atoms (Å × 10^3) for **2**[a]

Plane A	Ni, Fe, P1, P4 0.2947 X + 0.3804 Y + 0.8766 Z = 9.3653 Ni (−26), Fe (−21), P1 (24), P4 (24)
Plane B	Ni, P1, P2, C1 − 0.0915 X + 0.6426 Y − 0.7607 Z = 2.6324 Ni (−18), P1 (21), P2 (13), C1 (−17), C2* (−627)
Plane C	Ni, P3, P4, C4 0.6928 X − 0.5911 Y − 0.4132 Z = 4.9659 Ni (6), P3 (−4), P4 (−7), C4 (5), C3* (676)
Dihedral angles	A – B = 63.3, A – C = 67.5, B – C = 74.9

[a]Equations of planes are in the form $AX + BY + CZ = D$, where X, Y, and Z are the coordinates in Å, referred to orthogonal axes. Displacements are given in parentheses. Asterisks mark atoms not included in the plane calculation.

Selected bond lengths and angles are reported in Tables 4 and 5. The e.s.d.s in bond lengths and angles were calculated by the variance/covariance method. Some least-squares planes for **2** are reported in Table 6. See also 'Supplementary Material'.

Results and Discussion

Synthesis and Spectroscopic Properties of New Complexes

Reaction of $Li_2[(NO)_2\overline{Fe(\mu\text{-}PPh_2)(\mu\text{-}NO)}Fe(NO)(PPh_2)]$ with $CpCo(CO)I_2$ in THF at −78 °C followed by gradual warming to room temperature and work-up including chromatography on alumina afforded $(NO)_2\overline{Fe(\mu\text{-}PPh_2)(\eta^2\text{-}(Co,P)\text{-}\mu\text{-}Co(Cp)(CO)PPh_2)}Fe(NO)_2$ (**1**) as a dark brown solid in 24%

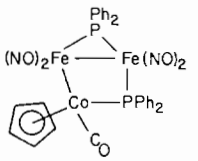

1

yield. The product readily decomposes in air to give $Fe_2(NO)_4(\mu\text{-}PPh_2)_2$ and an uncharacterized cobalt-containing material. Low stability of **1** in solution may be responsible for the isolation of $Fe_2(NO)_4(\mu\text{-}PPh_2)_2$ in *c.* 20% yield as a second major product from the reaction mixture. It probably also accounts for our inability to obtain good elemental analysis.

Spectroscopic properties of **1** are, in general, very much in accord with the structure elucidated by X-ray crystallography (*vide infra*). Thus, the FAB mass spectrum shows a parent ion peak at *m/e* 754, with fragment ions corresponding to stepwise loss of the CO and Cp groups and ejection of Co before dissociation of the NO ligands. Interestingly, this behavior parallels the mode of decomposition of **1** to $Fe_2(NO)_4(\mu\text{-}PPh_2)_2$ in solution. In the IR spectrum of **1**, a ν(CO) band is observed at 1980 cm^{-1}, and ν(NO) bands at 1750 and 1730 cm^{-1}. The latter two occur essentially at the same frequencies as the two intense ν(NO) bands of $(NO)_2\overline{Fe(\mu\text{-}PPh_2)(\eta^2\text{-}(C,P)\text{-}\mu\text{-}CH(R)PPh_2)}Fe(NO)_2$ (R = H, Me) [3], indicating that the bridging ligands η^2-(*Co,P*)-μ-Co(Cp)(CO)PPh_2 and η^2-(*C,P*)-μ-CH(R)PPh_2 exert very similar electronic effects on the $Fe(NO)_2$ groups. The ^1H NMR spectrum of **1** is unexceptional, consisting of the signals of the Ph and Cp protons at δ 7.50 and 5.24 ppm, respectively.

In agreement with the structure, the $^{31}P\{^1H\}$ NMR spectrum of **1** shows two resonances as doublets at δ 229.44 and 101.81 ppm, with $^2J(^{31}P^{31}P)$ = 49.4 Hz. The position of the lower-field resonance strongly points to the presence of metal–metal bonding that supports a bridging PPh_2 ligand [13]; this signal is accordingly assigned to the $\overline{Fe(\mu\text{-}PPh_2)}Fe$ phosphorus. The higher-field doublet is assigned to the $Fe(\mu\text{-}PPh_2)Co$ phosphorus because of its broad shape owing to quadrupolar coupling with the ^{59}Co nucleus [14]. This resonance is still positioned in the range associated with bridging PR_2 ligands that occur in conjunction with metal–metal bonding, although the X-ray analysis of **1** clearly reveals no Fe–Co interaction (*vide infra*). Thus, the present spectrum provides yet another exception to the generally useful empirical rule that low-field and high-field ^{31}P chemical shifts of μ-PR_2 are associated, respectively, with the presence and absence of metal–metal bonding [15].

An attempt was made to replace the CO ligand in **1** with PPh_3 to study possible effects of the substitution on structure and ^{31}P NMR spectrum. However, reaction of **1** with PPh_3 in THF at room temperature resulted in extensive decomposition and afforded $Fe_2(NO)_4(\mu\text{-}PPh_2)_2$ as the only characterized product. It would appear that substitution reactions of **1** may be severely limited by the low stability of the parent complex in solution.

The complex $Li_2[(NO)_2\overline{Fe(\mu\text{-}PPh_2)(\mu\text{-}NO)}Fe(NO)(PPh_2)]$ was also allowed to react with Ni(dppe)I_2 under the conditions that mirrored those for the

corresponding reaction with $CpCo(CO)I_2$. A similar work-up including chromatography on alumina led to the isolation of $(NO)_2Fe(1\text{-}(\mu\text{-}PPh)\text{-}2\text{-}(PPh_2)C_2H_4)_2Ni$ (2) as a dark purple solid in 20% yield. Also obtained in 10% yield, was $Fe_2(NO)_4(\mu\text{-}PPh_2)_2$. As in the reaction with $CpCo(CO)I_2$, extensive decomposition was noted.

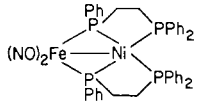

2

Spectroscopic data on 2 are consistent with its surprising heterobinuclear structure. Thus, the presence of a $Fe(NO)_2$ group is indicated by two intense IR ν(NO) bands at 1760 and 1710 cm^{-1}. In the $^{31}P\{^1H\}$ NMR spectrum, signals occur at δ 206.66 and 39.86 ppm as approximately 1:2:1 triplets, with $^2J(^{31}P^{31}P) = 10$ Hz. The former triplet is assigned to the equivalent μ-PPh phosphorus nuclei, and its position suggests the presence of metal–metal bonding [13]. The latter triplet is due to the equivalent CH_2PPh_2 phosphorus nuclei. The spectrum is typical of an AA'XX' spin system where $J(AX = A'X') = J'(AX' = A'X)$ [16].

The formation of 1 as a stable complex is predicted by isolobal analogy between RCH and Cp-Co(CO) [4]. This product becomes a new member of a class of mixed carbonyl–nitrosyl metal clusters. Such clusters are still relatively rare, and most of them represent homonuclear complexes of the second- and third-row transition metals [17]. By way of contrast, the isolation of 2 comes as a surprise. It is possible that a trinuclear Fe_2Ni product, I,

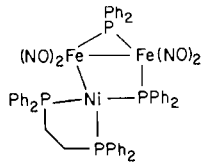

I

did form initially in the reaction but then decomposed to 2 and $Fe_2(NO)_4(\mu\text{-}PPh_2)_2$, which was also isolated. The formation of 2 from $[(NO)_2Fe(\mu\text{-}PPh_2)(\mu\text{-}NO)Fe(NO)(PPh_2)]^{2-}$ and $Ni(dppe)I_2$ requires loss of a Ph group from the diphosphine; it is surprising that such dephenylation occurs under the non-forcing experimental conditions employed in this synthesis. Since considerable decomposition occurs in the reaction and the product 2 shows only marginal stability, it would not be fruitful to study this transformation further.

We tried to extend the range of new heteronuclear metal complexes derived from $Li_2[(NO)_2Fe(\mu\text{-}PPh_2)(\mu\text{-}NO)Fe(NO)(PPh_2)]$ and ML_nI_2 by reacting the former with Cp_2ZrI_2 under similar experimental conditions. A ^{31}P NMR spectrum of the reaction mixture before work-up revealed the presence of several phosphorus-containing species; however, after an attempted chromatographic separation on alumina, only $Fe_2(NO)_4(\mu\text{-}PPh_2)_2$ was obtained in adequate amount for characterization.

The foregoing initial preparative results would appear to indicate that the dianion $[(NO)_2Fe(\mu\text{-}PPh_2)(\mu\text{-}NO)Fe(NO)(PPh_2)]^{2-}$ has a synthetic potential for heteronuclear metal complexes. However, its usefulness in that role may be limited by what now seems to be marginal stability of the resulting products.

Crystallographic Studies of $(NO)_2Fe(\mu\text{-}PPh_2)(\eta^2\text{-}(Co,P)\text{-}\mu\text{-}Co(Cp)(CO)PPh_2)Fe(NO)_2$ (1) and $(NO)_2Fe(1\text{-}(\mu\text{-}PPh)\text{-}2\text{-}(PPh_2)C_2H_4)_2Ni$ (2)

An ORTEP plot of 1 is shown in Fig. 1. The skeleton of the molecule consists of an asymmetric triangular arrangement of the metal atoms with two PPh_2 ligands bridging the Fe(1), Fe(2) and Co, Fe(2) metal atom pairs.

The Fe(1)–Fe(2) and Co–Fe(1) distances of 2.797(1) and 2.569(1) Å, respectively, are consistent with single metal–metal bonds, satisfying the 18-electron rule. Co, Fe(2) and Fe(1), P(2) are at the non-bonding distances of 3.796(1) and 2.791(2) Å, respectively. Thus, the structure of the $CoFe_2P_2$ core may be described as deriving from the fusion of a three- and a puckered four-membered ring sharing the Fe–Fe edge. The Fe(1)–Co–P(2)–Fe(2) torsion angle is 37.8°.

The cobalt atom lies in the plane of the Fe(1)-Fe(2)P(1) ring, whereas P(2) is out of this plane, as shown by the torsion angles Co–Fe(1)–Fe(2)–P(1) and P(1)–Fe(1)–Fe(2)–P(2) of −176.9 and −156.4°, respectively. The geometry of the $Fe_2(NO)_4(\mu\text{-}PPh_2)$ moiety is quite similar to that found in $(NO)_2Fe(\mu\text{-}PPh_2)(\eta^2\text{-}(C,P)\text{-}\mu\text{-}CH_2PPh_2)Fe(NO)_2$ [3], where a CH_2 group replaces Co(Cp)(CO).

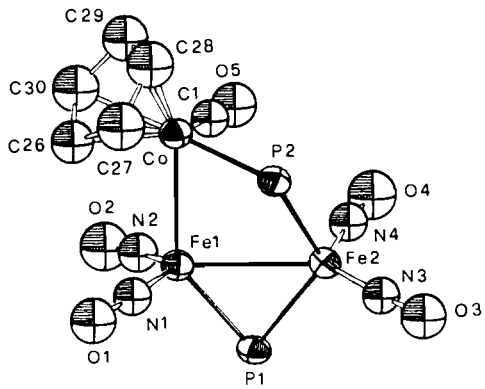

Fig. 1. ORTEP plot of 1, showing atom numbering scheme. Thermal ellipsoids are drawn at the 50% probability level. Carbon atoms of the phenyl rings (C(2)–C(7) and C(8)–C(13) at P(1), C(14)–C(19) and C(20)–C(25) at P(2)) are omitted for clarity.

TABLE 7. Bond distances (Å) and angles (°) in some $Fe_2L_n(\mu\text{-}PPh_2)(\mu\text{-}X)$ complexes with metal–metal bond[a]

Complex		Fe–Fe	Fe–P–Fe	Fe–P	Reference
L_n	X				
$(CO)_6$	PPh_2	2.623(2)	71.95(7)	2.233(6)	19
$(CO)_5(PMePh_2)$	OCMe	2.659(6)	74.15(7)	2.205(8)	20
$(NO)_4$	PPh_2	2.70(2)	74.5(5)	2.230(2)	21
$(CO)_6$	$P(Ph_2)C(CN)PPh_2$	2.727(1)	76.10(3)	2.21(2)	22
$(CO)_5(\eta^3\text{-}C_3H_5)(PPh_2C_3H_5)$	(no μ-X)	2.802(2)	79.0(1)	2.20(3)	23
$(CO)_6$	$CH(CN)PPh_2$	2.807(7)	78.0(3)	2.231(7)	22
$(NO)_4$	CH_2PPh_2	2.82(2)	78.4(8)	2.23(1)	3

[a]Average values are given when structurally equivalent data are available.

The Fe–Fe bond length in bridged binuclear complexes shows a great variability, depending on the nature of the bridging atoms and the stereochemistry of the ligand system [13b, 18]. Table 7 reports data for several binuclear complexes in which the Fe–Fe bond is supported by at least one μ-PPh_2; Carty [13b] has compiled some corresponding data for a number of related $Fe_2(CO)_6(\mu\text{-}PPh_2)(\mu\text{-}X)$ complexes. Inspection of the reported Fe–Fe distances shows that they vary over a rather wide range, from 2.548(1) Å in $(CO)_3Fe(\mu\text{-}PPh_2)(\mu\text{-}CC(Cy_2PH)Ph)Fe(CO)_3$ [13b] to 2.82(2) Å in $(NO)_2Fe(\mu\text{-}PPh_2)(\eta^2\text{-}(C,P)\text{-}\mu\text{-}CH_2PPh_2)Fe(NO)_2$ [3]. The Fe–P distances, on the other hand, display much less variation. This is reflected in the widening (*c.* 8.5°) of the Fe–P–Fe bond angle as the Fe–Fe distance increases from 2.55 to 2.82 Å.

Unfortunately, available structural data are not sufficient to rationalize the observed trends in the metal–metal and metal–phosphorus distances, for the general lack of strictly related compounds. Furthermore, theoretical calculations have been performed only for the simplest compounds [24], and the results are not directly extendable to more complicated systems.

It is interesting to observe that in the trinuclear complex **1**, the values of the Fe–P(1) distances (av. 2.22(3) Å) are well in the range reported in Table 7, while the Fe(2)–P(2) distance of 2.291(2) Å is markedly longer. This value is closer to that of 2.28(1) Å found in $[Na(2,2,2\text{-crypt})]_2[Fe_2(CO)_6(\mu\text{-}PPh_2)_2]$ [19], where there is no metal–metal bonding interaction.

At present, it is not possible to assess whether the difference between the two Fe–P distances is related to the bonding–non-bonding situation of the Fe(1), Fe(2) and Co, Fe(2) metal pairs, or to other effects. In fact, the Co–P(2) distance of 2.191(2) Å is not lengthened with respect to the values found for Co–P distances in binuclear cobalt complexes having a metal–metal bond, e.g. $Cp_2Co_2(\mu\text{-}PPh_2)_2$ (av. 2.16 Å) [25] and $Co_2(CO)_2(NO)_2(\mu\text{-}PPh_2)_2$ (av. 2.191(2) Å) [21].

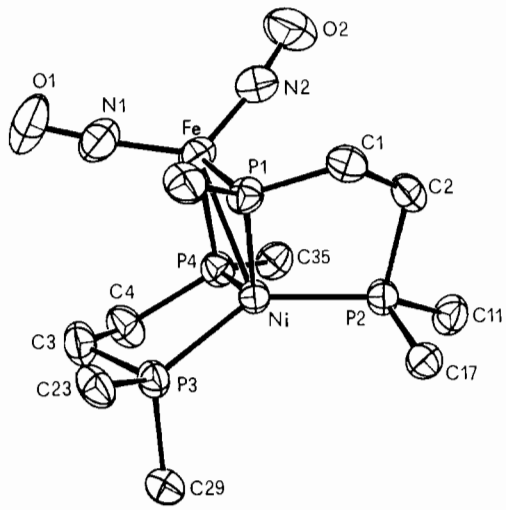

Fig. 2. ORTEP plot of **2**, showing atom numbering scheme. Thermal ellipsoids are drawn at the 50% probability level. Only the ipso-carbon atoms of the phenyl rings are given for clarity (carbon atoms of each phenyl ring: C(5)–C(10) at P(1), C(11)–C(16) and C(17)–C(22) at P(2), C(23)–C(28) and C(29)–C(34) at P(3), C(35)–C(40) at P(4)).

The Co–Fe(1) bond length of 2.569(1) Å is shorter than those found in FeCo bridging-phosphido polynuclear complexes, in which the Fe–Co distance ranges from 2.597(2) to 2.724(2) Å [26]. Anyhow, it compares well with the average value of 2.555 Å given in the literature [27]. The orientation of the CO and Cp ligands coordinated to Co is determined by steric interactions with the phenyl groups at P(2).

The crystal structure of **2** consists of discrete molecules (Fig. 2) in which one $Fe(NO)_2$ group is bonded to a Ni atom by the bridging of two PPh-$(CH_2CH_2PPh_2)$ ligands. The phosphine P atoms coordinate to the nickel atom, giving rise to two five-membered rings with an envelope conformation. The dihedral angle between the planes defined by the Ni, P(1), P(2), C(1) fragment (coplanar within 0.04 Å) and the Ni, P(3), P(4), C(4) fragment (coplanar within 0.014 Å) is 97.4°. These planes lie

on opposite sides of the central $\overline{FeNiP(1)P}(4)$ ring, forming dihedral angles of 63.3 and 67.5°, respectively, with the latter.

The $\overline{FeNiP(1)P}(4)$ ring is essentially planar (±0.026 Å), resembling the structures of $Ni_2(CO)_4(\mu\text{-}PPh_2)_2$ [28], $Fe_2(NO)_4(\mu\text{-}PPh_2)_2$ [21], $Co_2(CO)_2(NO)_2(\mu\text{-}PPh_2)_2$ [21], and $Fe_2(NO)_4(\mu\text{-}P(CF_3)_2)_2$ [29], where similar planar rings have been found. Planar core structures have been also observed in $[Na(2,2,2\text{-crypt})]_2[Fe_2(CO)_6(\mu\text{-}PPh_2)_2]$ [19] and $Cp_2Ni_2(\mu\text{-}PPh_2)_2$ [25], where there are no metal–metal bonding interactions.

The coordination polyhedron about each metal atom may be described as a highly distorted trigonal bipyramid where P(1) and P(4) occupy pseudoaxial positions, if the metal atoms are considered to occupy discrete coordination sites. In fact, Fe is coplanar with Ni, N(1), and N(2) whereas Ni is coplanar with Fe, P(2), and P(3), as shown by the sums of bond angles around Fe and Ni of 359.9 and 360.0°, respectively.

The Fe–Ni bond distance of 2.6166(4) Å is reasonable for a single Fe–Ni bond in this type of complexes, being intermediate between the values of 2.515(2) and 2.70(2) Å found in $Ni_2(CO)_4(\mu\text{-}PPh_2)_2$ [28] and $Fe_2(NO)_4(\mu\text{-}PPh_2)_2$ [21], respectively.

It is noteworthy that the Ni–P(phosphine) distances (av. 2.16(1) Å) are longer than the Ni–P(phosphido) distances (av. 2.115(7) Å), as already observed in other binuclear complexes [3]. However, the latter value is significantly lower than that found in $Ni_2(CO)_4(\mu\text{-}PPh_2)_2$ (av. 2.191(8) Å) [28]. By contrast, the Fe–P bond lengths (av. 2.285(5) Å), are markedly greater than those reported in Table 7, approaching the value of 2.291(2) Å found in **1** for the Fe(2)–P(2) distance.

Supplementary Material

Anisotropic thermal parameters, hydrogen atom parameters and structure factor lists are available from the authors.

Acknowledgements

We gratefully acknowledge financial support of the National Science Foundation (through Grant CHE-8420806 to A.W.), Ministero Pubblica Istruzione (Rome), and NATO (through Grant 0.68.81 to A.W. and M.C.). FAB mass spectra were obtained at the Ohio State University Chemical Instrument Center (funded in part by National Science Foundation Grant 79-10019).

References

1 A. Wojcicki, *Inorg. Chim. Acta, 100* (1985) 125.
2 Y.-F. Yu, C.-N. Chau and A. Wojcicki, *Inorg. Chem., 25* (1986) 4098.
3 C.-N. Chau, Y.-F. Yu, A. Wojcicki, M. Calligaris, G. Nardin and G. Balducci, *Organometallics, 6* (1987) 308.
4 R. Hoffmann, *Angew. Chem., Int. Ed. Engl., 21* (1982) 711.
5 D. F. Shriver, *The Manipulation of Air-Sensitive Compounds*, McGraw-Hill, New York, 1969.
6 D. D. Perrin, W. L. F. Armarego and D. R. Perrin, *Purification of Laboratory Chemicals*, Pergamon, Oxford, U.K., 1966.
7 R. B. King, *Inorg. Chem., 5* (1966) 82.
8 A. F. Reid and P. C. Wailes, *J. Organomet. Chem., 2* (1964) 329.
9 G. R. Van Hecke and W. DeW. Horrocks, Jr., *Inorg. Chem., 5* (1966) 1968.
10 T. B. Rauchfuss and T. D. Weatherwill, *Inorg. Chem., 21* (1982) 827.
11 *International Tables for X-Ray Crystallography*, Vol. IV, Kynoch, Birmingham, U.K., 1974.
12 B. A. Frenz, *Enraf-Nonius Structure Determination Package*, Enraf-Nonius, Delft, The Netherlands, 1980.
13 (a) P. E. Garrou, *Chem. Rev., 81* (1981) 229; (b) A. J. Carty, *Adv. Chem. Ser., 196* (1982) 163.
14 S. Aime, L. Milone and M. Valle, *Inorg. Chim. Acta, 18* (1976) 9.
15 A. J. Carty, S. A. MacLaughlin and D. Nucciarone, in J. G. Verkade and L. D. Quin (eds.), *Phosphorus-31 NMR Spectroscopy in Stereochemical Analysis: Organic Compounds and Metal Complexes*, VCH Publishers, Deerfield Beach, FL, 1986, pp. 559–619.
16 L. M. Jackman and S. Sternhell, *Applications of Nuclear Magnetic Resonance Spectroscopy in Organic Chemistry*, Pergamon, Oxford, U.K., 2nd edn., 1969, pp. 134–139.
17 W. L. Gladfelter, *Adv. Organomet. Chem., 24* (1985) 41.
18 H. Vahrenkamp, *Angew. Chem., Int. Ed. Engl., 17* (1978) 379.
19 R. E. Ginsburg, R. K. Rothrock, R. G. Finke, J. P. Collman and L. F. Dahl, *J. Am. Chem. Soc., 101* (1979) 6550.
20 Y.-F. Yu, J. Gallucci and A. Wojcicki, *J. Am. Chem. Soc., 105* (1983) 4826.
21 E. Keller and H. Vahrenkamp, *Chem. Ber., 112* (1979) 1626.
22 Y.-F. Yu, A. Wojcicki, M. Calligaris and G. Nardin, *Organometallics, 5* (1986) 47.
23 Y.-F. Yu, J. Gallucci and A. Wojcicki, *J. Chem. Soc., Chem. Commun.*, (1984) 653.
24 (a) J. K. Burdett, *J. Chem. Soc., Dalton Trans.*, (1977) 423; (b) B. K. Teo, M. B. Hall, R. F. Fenske and L. F. Dahl, *Inorg. Chem., 14* (1975) 3103.
25 (a) H. Vahrenkamp and E. Keller, *Chem. Ber., 112* (1979) 2347; (b) H. Vahrenkamp, E. J. Wucherer and
26 D. Wolters, *Chem. Ber., 116* (1983) 1219.
D. A. Roberts and G. L. Geoffroy, in G. Wilkinson, F. G. A. Stone and E. W. Abel (eds.), *Comprehensive*
27 *Organometallics Chemistry*, Pergamon, Oxford, U.K., 1982, Ch. 40.
28 J. A. J. Jarvis, R. H. B. Mais, P. G. Owston and D. T. Thompson, *J. Chem. Soc. (A)*, (1970) 1867.
29 W. Clegg, *Inorg. Chem., 15* (1976) 2928.